An-Najah University Journal for Research – A
Natural Sciences

Advanced Oxidation of Organic Dyes Using a Porous Gold Electrode: Kinetic Analysis

Fatima Zaaboul[1,*], Chaimaa Haoufazane[2], Mohamed EL Ouardi[3], Meryem Abouri[3], Khalil Azzaoui[4,5], Belkheir Hammouti[6], Badr Eddine Kartah[2], Shehdeh Jodeh[7,*] & Abderrahim El Hourch[1,*]

(Type: Full Article). Received: 7th Mar. 2025, Accepted: 20th Apr. 2025. Accepted: 1st Feb. 2026,
DOI: https://doi.org/10.35552/anujr.a.40.1.2476

Abstract: **MAX 250 words** This study evaluates the efficiency of anodic oxidation processes for the degradation of the azo dye Reactive Blue 203 (RB203) using a gold electrode in an compartmented electrochemical cell. Unlike most studies that rely on conventional electrodes such as BDD or graphite, this work explores the use of a porous gold electrode—an uncommon yet promising material in dye degradation—highlighting its high electrocatalytic activity and exceptional chemical stability. Experiments explored the effects of current density, initial pH and type of supporting electrolyte. The gold electrode performed remarkably well, achieving a 91.82% decolorization rate and 96% Chemical Oxygen Demand (COD) removal after 360 minutes of treatment. Best performance was observed under acidic conditions (pH = 3), where the formation of hydroxyl radicals (•OH) is favored. The use of KCl as a supporting electrolyte improved degradation compared to Na_2SO_4, thanks to better ionic conductivity and the generation of reactive species such as Cl_2 and HOCl. Kinetic analysis revealed that the reaction follows a pseudo-first-order model, with rate constants increasing from 0.00261 min-¹ to 0.0141 min-¹ as the current density increases from 100 to 400 mA.cm-². These results confirm that anodic oxidation, with the gold electrode, is an effective and sustainable method for treating textile wastewater.

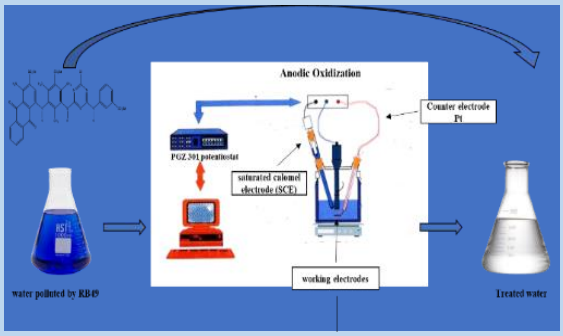

Keywords: Anodic Oxidation, Reactive Blue 203, Azo Dye Degradation, Gold Electrode, Electrochemical Treatment, Textile Wastewater.

Introduction

The textile industry is a major source of untreated wastewater discharges, which have adverse effects on aquatic ecosystems and human health [1-3]. These wastewaters, rich in synthetic dyes with diverse color structures and intensities, are complex and make it difficult to treat them efficiently and economically [4, 5] To meet these challenges, various approaches have been implemented, such as adsorption [6-8] , biological treatment [9-12], membrane separation [13, 14] and coagulation/flocculation [15, 16]. Among emerging solutions, electrochemical advanced oxidation processes (EAOP) show particular promise for removing organic pollutants, offering an efficient and compact technology that has attracted growing interest over the past decade [17, 18].

Electrochemical advanced oxidation processes (EOAP) are distinguished by their speed and efficiency in treating organic pollutants, while avoiding the secondary pollution associated with the use of chemicals [19, 20]. These processes rely on the generation of hydroxyl radicals (.OH), which ensure the complete decomposition of organic matter into carbon dioxide (CO_2) and water (H_2O) [21]. Among these techniques, electrocatalytic oxidation is attracting growing interest due to its ability to degrade a wide range of organic pollutants [22]. The effectiveness of EOAP depends heavily on the choice of anode materials, which play a key role in oxidation mechanisms [23]. These mechanisms include direct oxidation, where electrons are transferred directly from the contaminant to the anode surface, and indirect oxidation, in which electroactive species generated by the anode participate in pollutant degradation [24]. The main indirect oxidation mechanism is based on the formation of hydroxyl radicals via the discharge of water molecules at the anode surface, as shown in equation (1) [25]. These hydroxyl radicals then interact with organic matter and its intermediates, leading to their mineralization into inorganic products such as carbon dioxide (CO_2) and water (H_2O) (equations 2 and 3) [26]:

1 Laboratory of Materials, Nanotechnologies and Environment, Faculty of Sciences, Mohammed V University in Rabat, Avenue Ibn Battouta, Rabat BP1014, Morocco.
* Corresponding author email: zaaboul.fatima00@gmail.com
2 Laboratory of Plant Chemistry, Organic and Bioorganic Synthesis, Faculty of Sciences, Mohammed V University in Rabat, 4 Avenue Ibn Battouta, BP, P.O. Box 1014, Rabat 10090, Morocco
3 Laboratory of Spectroscopy, Molecular Modeling, Materials, Nanomaterial, Water and Environment, Faculty of Sciences, Mohammed V University in Rabat, Avenue Ibn Battouta, Rabat BP1014, Morocco
4 Engineering Laboratory of Organometallic, Molecular Materials and Environment, Faculty of Sciences, Sidi Mohamed Ben Abdellah University, 30000 Fez, Morocco;
5 Laboratory of Industrial Engineering, Energy and the Environment (LI3E) SUPMTI, Rabat, Morocco
6 Euromed University of Fes, UEMF, Fes, Morocco
7 Department of Chemistry, An-Najah National University, Nablus P.O. Box 7, Palestine.

$M + H2O \rightarrow M(OH\cdot) + H+ + e-$ (1)

$M(OH\cdot) + \text{Organic matter} \rightarrow M + \text{Intermediates}$ (2)

$M(OH\cdot) + \text{Intermediates} \rightarrow M + CO2 + H2O + \text{Inorganic ion}$ (3)

The working electrode plays a central role in the efficiency of electrochemical processes, directly influencing the degradation performance of organic pollutants [27]. Anodic electrodes catalyze the oxidation reactions required for the decomposition of dyes and other contaminants [28]. In this study, the gold electrode was used and examined to assess its performance in the electrochemical degradation of textile dyes [29] . The gold electrode has been selected for its exceptional corrosion resistance, high electrical conductivity, and remarkable electrocatalytic properties, which make it an attractive candidate for electrochemical advanced oxidation processes. These characteristics ensure not only long-term operational stability in acidic and oxidizing environments, but also high efficiency in generating hydroxyl radicals (•OH), which are crucial for the complete degradation of complex organic molecules such as azo dyes. While several anodic materials such as boron-doped diamond (BDD), graphite, or titanium-based electrodes have been extensively studied for dye degradation, the application of gold electrodes in this context remains extremely limited, mainly due to economic considerations. However, their physicochemical advantages could outweigh these limitations, particularly in research contexts seeking high-performance and model systems. This study thus aims to fill this gap by investigating the electro catalytic behavior of a porous gold electrode toward the degradation of Reactive Blue 203 (RB203), and to evaluate its potential as a reliable and efficient alternative to conventional materials for sustainable wastewater treatment [30].

This study aims to evaluate the effectiveness of an electrochemical oxidation process for removing a commonly used textile dye. To this end, the azo dye Reactive Blue 203 (RB203) ($C_{28}H_{29}N_5O_{21}S_6$-4Na) was selected as the model contaminant [31]. This choice makes it possible to examine in detail the electrochemical activity of the electrodes used in the

electrocatalytic oxidation process. Its chemical structure is illustrated in **Figure 1** and its chemical characteristics are listed in **Table 1**.

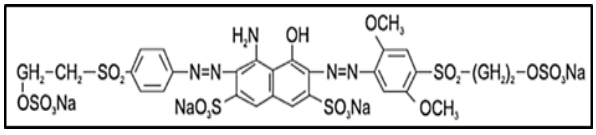

Figure (1): Chemical structure of RB203.

Table (1): Chemical characteristics of the dye used.

Colorant used	Gross formula	Molar mass (g/mol)	Solubility in water	λmax (nm)
Reactive Bleu 203	$C_{28}H_{29}N_5O_{21}S_64Na$	1051.87	Elevated	605

Materials and Methods

Materials

Potassium chloride KCl (99.0%) and sodium hydroxide NaOH (99.0%) were supplied by VWR Prolabo Chemicals. Sodium sulfate Na_2SO_4 (99.0%) and sulfuric acid H_2SO_4 (96.0%) were supplied by Panreac.

Electro-oxidation experiments:

RB203 electrolysis was carried out to evaluate the electrocatalytic oxidation activity of the electrodes used. The experiments were carried out using a PGZ 301 potentiostat electrochemical cell in a non-compartmentalized electrochemical reactor. This procedure involves the use of a three-electrode system, where a platinum electrode acts as counter electrode, a calomel saturated electrode (SCE) serves as reference electrode, and gold working electrode are used as working electrodes. The experimental setup of the electrochemical decolorization system is illustrated in **Figure 2**.

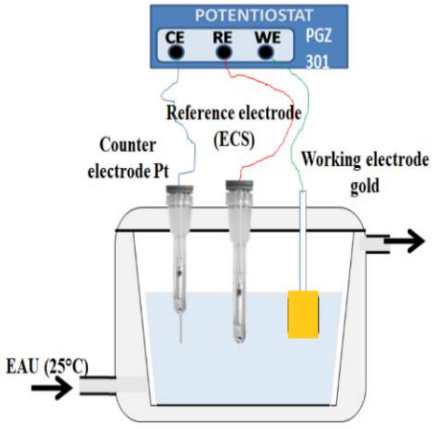

Figure (2): Schematic diagram of the anodic oxidation experimental set-up.

The experimental solution contained RB203 at a concentration of 100 mg/l, with an electrolyte support of Na_2SO_4 and KCl (0.2 M). Sulfuric acid and sodium hydroxide were used for pH adjustment. Throughout the experiments, the solution was stirred using a magnetic stirrer, while maintaining an ambient temperature of 20°C for a period of 180 minutes.

Table (2): Summary table of effects studied, their fixed and various parameters for oxidation.

Effects studied	Fixed parameters	Varied parameters
Effect of current density	Initial concentration: 40 mg/L Volume: 50 mL Electrolyte: Na_2SO_4 (0,2 M) Colorant pH: 6.63 Time: 3h	Density of current $mA.cm^{-2}$: 100; 200; 300; 400
Effect of pH	Initial concentration: 40 mg/L Volume: 50 mL Electrolyte: Na_2SO_4 (0,2M) Density of current: 300 $mA.cm^{-2}$ Time: 3h	pH: 3; 5; 6,63; 9; 11
Electrolyte effect	Initial concentration: 40 mg/L Volume: 50 mL Colorant pH: 6.63 Density of current: 300 $mA.cm^{-2}$ Time: 3h	Electrolyte: KCl (0,2 M)

Analytical methods

The degradation rate was calculated from the concentration of samples taken at time (5 min, 10 min, 15 min, 30 min, 60 min, 120 min, 180 min) by measuring absorbance at the maximum visible absorption wavelength (605 nm), using a UV-Vis spectrophotometer. The degradation rate was calculated as follows:

$$\%R = \frac{(C_0 - C_e)}{C_0} \times 100 \quad (4)$$

Where C_0 and C_t are the absorbance values at an initial time and at time t, respectively.

The expression of the velocity is proportional to the concentration C of the dye RB203:

$$v = -\frac{dC}{dt} = k.\ C \quad (5)$$

By integrating the above equation (with $C = C_0$ at $t = 0$), we obtain:

$$\ln(\frac{C}{C_0}) = -k.t \quad \text{ou} \quad \ln(\frac{C_0}{C}) = k.t \quad (6)$$

The rate constant k is determined graphically, as it is the slope of the straight-line ln (C_0/C) vs t and is expressed in inverse units of time (min^{-1}).

The titrimetric method using dichromate in acid medium as the oxidizing agent was adopted to quantify COD. To assess the efficiency of COD removal, we applied the following formula:

$$\text{COD (\%)} = \frac{COD_0 - COD_t}{COD_0} . 100\% \quad (7)$$

where DCO_0 is the COD of the initial concentration and DCO_t is the COD at the specified time t.

Results and Discussion

Effect of electrolyte on OR

Cyclic voltammograms obtained on the or electrode highlight the electrochemical behavior of RB203 dye in two different electrolyte media: sulfuric acid (H_2SO_4 1.0 M) and sodium hydroxide (NaOH 0.1 M). In an acidic medium (**Figure 3**), the curve in the absence of RB203 (black curve) shows a typical background current, reflecting the electrochemical activity of the electrode in H_2SO_4 [32]. The addition of RB203 (red curve) results in a significant increase in current density, as well as the appearance of anodic and cathodic peaks, reflecting redox processes linked to the electrochemical transformation of dye functional groups, such as azo groups (-N=N-). The high current density indicates an effective interaction between RB203 molecules and the electrode in an acidic environment, favoring electron transfer [33, 34].

In the basic medium (Figure 3b), the curve in the absence of RB203 shows a background current characteristic of 0.1 M NaOH. In the presence of RB203, variations in current densities and distinct peaks are observed, although the latter are less marked than in the acidic medium. This suggests reduced electrochemical reactivity in the basic medium, probably due to deprotonation of dye functional groups, resulting in altered reaction kinetics at the electrode.

Comparison between the two media reveals greater electrochemical activity of RB203 dye in acidic conditions, where higher oxidative currents suggest better compatibility of acidic conditions for electrochemical degradation processes. These results underline the importance of the choice of electrolytic medium for optimizing the electrochemical degradation performance of RB203 dye [35].

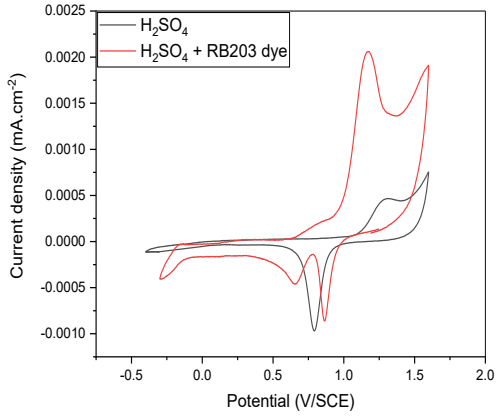

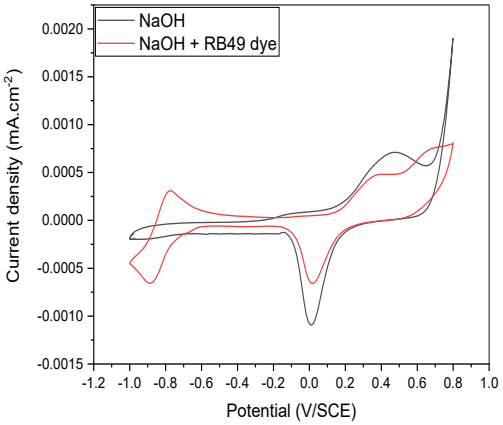

Figure (3): Cyclic voltammograms plotted on the Gold electrode at 100 mV/s of 10 mM Rb203 dye in: (a) H_2SO_4 (1.0 M) and (b) NaOH (0.1 M).

Effect of current density

Exploring the impact of applied current density is a key element in the evaluation of RB203 solution discoloration by anodic oxidation. Various research studies have highlighted the influence of applied current on the efficiency of the electrochemical process [36]. **Figure 4** shows the influence of different applied current densities (from 100 to 400 $mA.cm^{-2}$) on discoloration over time during electrolysis of RB203 (0.1 mM) with Na_2SO_4 (0.1 M), conducted at room temperature (20°C) and natural pH, using an ore electrode.

The results obtained showed that as the current density increased, so did the rate of dye degradation. At current densities of 300 and 400 $mA.cm^{-2}$, 82% and 91.82%, respectively, of dye degradation were observed after 180 minutes of electrolysis, while it was 37.81% and 63% at current densities of 100 and 200 mA.cm-2, respectively. This is probably explained by the fact that the rate of •OH radical generation increases with current density [37] .

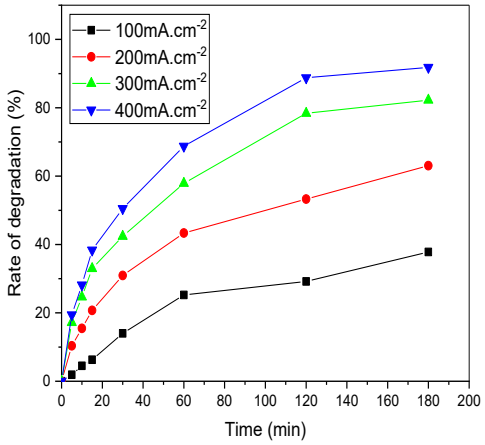

Figure (4): Effect of current density on the rate of degradation of RB203 dye ([RB203] = 40 mg/L, V = 50 mL, [Na_2SO_4] = 0.2 M, pH = 6.63, t = 180 min).

The curves shown in **Figure 5** and the data in Table 4 demonstrate the effect of current density on dye degradation kinetics during electrolysis. By increasing the current density from 100 to 400 $mA.cm^{-2}$, we observe a progressive improvement in the coefficients of determination (R^2), rising from 0.93284 to 0.96567. These high coefficients of determination (close to 1) indicate that the kinetic models used to analyze the data fit the

experimental results well. At the same time, velocity constants (k) increase significantly with current density, from 0.00261 min^{-1} to 0.0141 min^{-1}. This trend shows that higher current densities accelerate dye degradation. The shape of the disappearance kinetics curves shows that the rate of oxidation reaction by the anodic oxidation process follows pseudo-first-order kinetics.

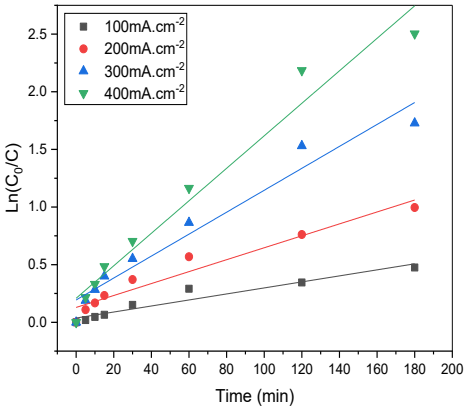

Figure (5): Effect of current density on the degradation kinetics of RB203 dye ([RB203] = 40 mg/L, V = 50 mL, [Na_2SO_4] = 0.2 M, pH = 6.63, t = 180 min).

Table (3): Coefficients of determination (R^2) and rate constants (k) for different current densities.

Density of current ($mA.cm^{-2}$)	100	200	300	400
R^2	0,93284	0,94313	0,95388	0,96567
k (min^{-1})	0,00261	0,00518	0,00952	0,0141

Effect of initial pH

pH adjustment plays a crucial role in the wastewater treatment process during anodic oxidation. There are various reports on the influence of pH, however, conclusions vary and may even be contradictory due to the different organic and electrode molecules involved. A series of experiments was carried out using a set of solutions of RB203 at a concentration of 0.1 mM, with pH variations between 3 and 10 [38] .

The pH values of the solutions were modified by introducing drops of H_2SO_4 or NaOH. Figure 6 shows the influence of initial pH on the percentage of RB203 discoloration. According to the results shown in **Figure 6**, after 180 minutes of electrolysis, more than 89% of the degradation rate is obtained for pH values equal to 3 and 5. As the pH decreases, the medium becomes more acidic, increasing the concentration of protons (H^+). This acidity promotes the formation of hydroxyl radicals (•OH), which are highly effective in degrading dye molecules. In contrast, for pH values equal to 9 and 11, the degradation rate is 40.68% and 31.66% respectively as the proton concentration is low, reducing the formation of hydroxyl radicals and therefore the efficiency of dye degradation [39]. This explains why the degradation rate is much higher at acidic pH than at basic pH.

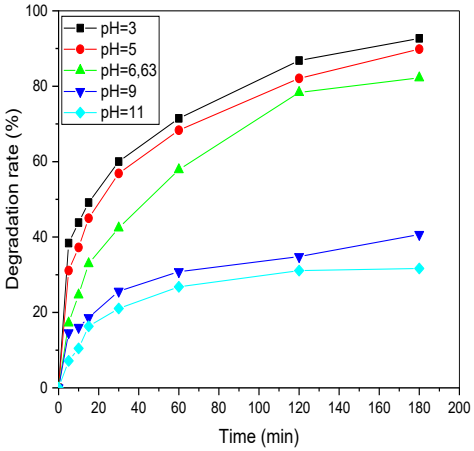

Figure (6): Effect of pH on the degradation rate of dye RB203 ([RB203] = 40 mg/L, V = 50 mL, [Na_2SO_4] = 0.2 M, t = 180 min, i = 300 $mA.cm^{-2}$).

The curves shown in **Figure 7** and the data in table 6 indicate that pH has a significant impact on dye degradation kinetics. The coefficients of determination (R^2) show a strong correlation for acidic and neutral media, but a reduced correlation for basic media. Rate constants (k) also decrease with increasing pH, from 0.01305 min^{-1} at pH 3 to just 0.00188 min^{-1} at pH 11. These results suggest that under acidic conditions, the production of hydroxyl radicals (•OH) is favored, accelerating dye degradation. On the other hand, in basic environments, the low proton concentration limits the formation of these radicals, thus slowing down the

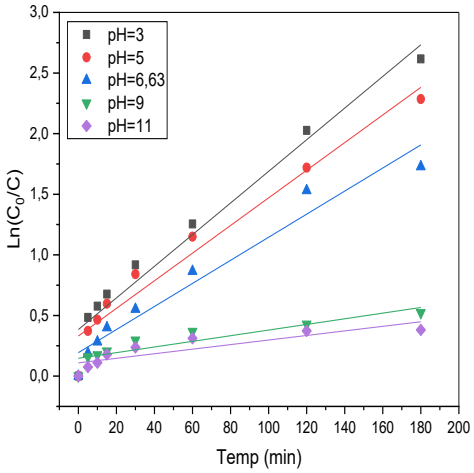

Figure (7): Effect of pH on degradation kinetics of dye RB203. ([RB203] = 40 mg/L, V = 50 mL, [Na_2SO_4] = 0.2 M, t = 180 min, i = 300 $mA.cm^{-2}$).

Table (4): Coefficients of determination (R^2) and rate constants (k) for different pH values.

pH	3	5	6,63	9	11
R^2	0,96017	0,95626	0,95388	0,81223	0,75100
k (min^{-1})	0,01305	0,0114	0,00952	0,00233	0,00188

Effect of electrolyte support

To demonstrate the effectiveness of decolorization, we explored the use of two supporting electrolytes, namely Na_2SO_4 and KCl, to assess their impact on the decolorization process at all three electrodes. The figure shows that the concentration of KCl exerts a significant influence on the rate of decolorization and the removal of organic substances compared with Na_2SO_4 for the electrode.

Figure 8 shows that the rate of dye degradation after 180 minutes is 82.23% with Na_2SO_4 as the supporting electrolyte, while it reaches 92.66% with KCl. This notable difference can be attributed to the properties of the supporting electrolytes. KCl, having better ionic conductivity, facilitates more efficient charge transfer and increased generation of reactive species (Cl_2) at the electrode surface ((8)-(9)), intensifying the dye degradation process. In contrast, Na_2SO_4, while effective, does not offer the same efficiency in forming the reactive species required for optimal degradation. Consequently, the use of KCl leads to a higher degradation rate compared to Na_2SO_4 under the same experimental conditions [40].

$$2\ Cl^- \rightarrow Cl_2 + 2e^- \quad (8)$$

$$Cl_2 + H_2O \rightarrow HOCl + H^+ + Cl^- \quad (9)$$

$$HOCl \leftrightarrow H^+ + OCl^- \quad (10)$$

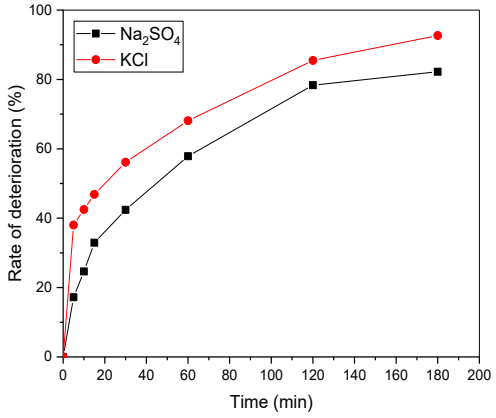

Figure (8): Effect of supporting electrolyte on degradation rate of dye RB 203 ([RB203] = 40 mg/L, V = 50 mL, [KCl] = 0.2 M, pH = 6.63, t = 180 min, i = 300 mA.cm^{-2}).

The data in **Table 5** and the shape of the curves in **Figure 9** show the impact of the supporting electrolyte on dye degradation kinetics. With Na_2SO_4 as the supporting electrolyte, the coefficient of determination (R^2) is 0.95388 and the rate constant (k) is 0.00952 min^{-1}. Using KCl as the supporting electrolyte, these values increase to 0.97027 for R^2 and 0.01295 min^{-1} for k. This indicates that KCl slightly improves the correlation between the kinetic model and experimental data, and increases the rate of dye degradation. This difference can be attributed to KCl better ionic conductivity and Cl_2 regeneration ((5)-(6)), which promotes more efficient generation of the reactive species required for dye degradation, compared with Na_2SO_4.

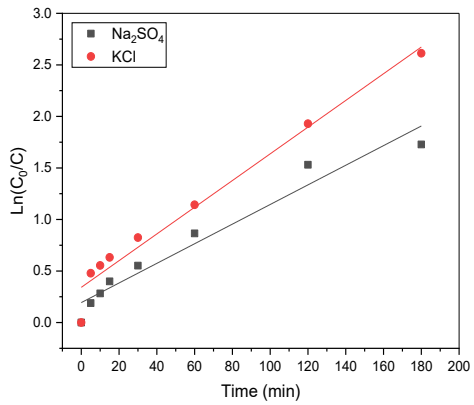

Figure (9): Effect of supporting electrolyte on RB 203 dye degradation kinetics ([RB203] = 40 mg/L, V = 50 mL, [KCl] = 0.2 M, pH = 6.63, t = 180 min, i = 300 mA.cm^{-2}).

Table (5): Coefficients of determination (R^2) and rate constants (k) for Na_2SO_4 and KCl as supporting electrolyte.

Electrolyte support	Na_2SO_4	KCl
R^2	0,95388	0,97027
k (min^{-1})	0,00952	0,01295

COD effect

Experiments were carried out to evaluate the effectiveness of the gold electrode (Gold) in the anodic oxidation process of RB203. The variation in Chemical Oxygen Demand (COD) was monitored during these experiments, and the results are shown in **Figure 10**. Based on these findings, it is notable that the reductions in Chemical Oxygen Demand (COD) with the gold anode (Gold) were considerably higher [41] [42] [43] . After 360 minutes of treatment, electrolysis with the gold anode virtually eliminated Chemical Oxygen Demand (COD) by 96%. These results indicate that the gold anode (Gold) demonstrates a significantly higher capacity to degrade RB203 **Fig 10.a**.

Figure 10b shows the kinetics of the anodic oxidation of RB203 on the gold anode. Analysis of the linear plot of ln(C_0/C) versus time reveals that RB203 degradation follows a first-order reaction, with a direct correlation to the percentage removal of Chemical Oxygen Demand (COD). Kinetic constants for COD elimination were determined to be 0.0077 min-1, for Gold anode, respectively (see **Table 6**).

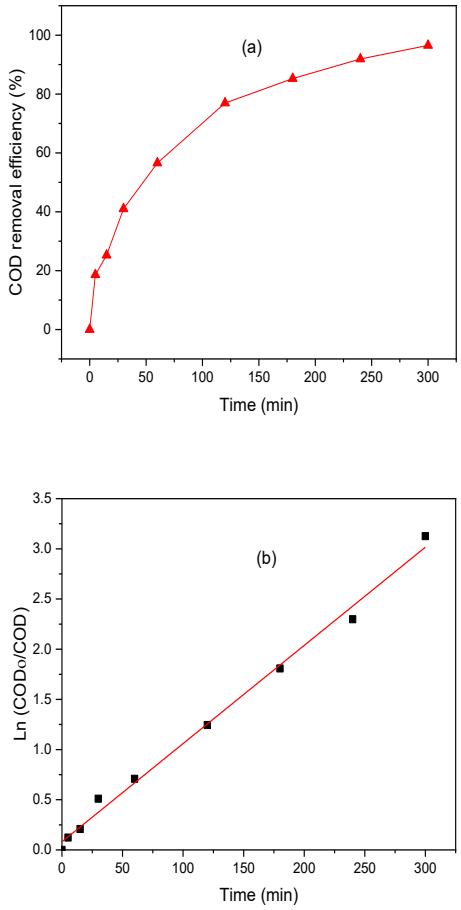

Figure (10): a Influence of COD elimination efficiency, b pseudofirst-order kinetics for RB203 decay (conditions: V= 0.05 L; [RB203] = 0.1 mM; T=20 °C; current density: 200 mA·cm^{-2}; electrolyte: 0.2 M Na_2SO_4).

Table (6): Kinetic constant of RB203 oxidation upon COD removal.

Electrode	K_{app} (min^{-1})	R^2
Gold	0.0077	0.99

Conclusion

This study demonstrated the effectiveness of anodic oxidation processes for the degradation of the azo dye Reactive Blue 203 (RB203) using a variety of electrodes and operating conditions. Among the electrodes tested, the gold (GOLD) electrode proved the most effective, achieving a 91.82% decolorization rate and 96% Chemical Oxygen Demand (COD) removal after 360 minutes of treatment. Parameters such as current density, initial pH and electrolyte type were optimized to maximize process efficiency. In particular, acidic conditions (pH = 3) and the use of KCl as the supporting electrolyte favored increased production of hydroxyl radicals (•OH), thus improving degradation performance. Kinetic analyses confirmed that the reaction follows a pseudo-first-order model with high kinetic constants and coefficients of determination. These results highlight the potential of anodic oxidation processes as a sustainable and efficient alternative for textile wastewater treatment, while underlining the need for further research for large-scale industrial applications.

Disclosure Statements

- **Ethics approval and consent to participate:** No applicable
- **Consent for publication:** No applicable
- **Availability of data and materials:** The raw data required to reproduce these findings are available in the body and illustrations of this manuscript.
- **Funding:** This research received no funding
- **Conflicts of interest:** On behalf of all authors, the corresponding author states that there is no conflict of interest.

Open Access

References

1] Ghanbari T, Abnisa F, Daud WMAW. A review on production of metal organic frameworks (MOF) for CO2 adsorption. Science of The Total Environment. 2020;707:135090.

2] Rais Z, Taleb M, Sfaira M, Filali Baba M, Hammouti B, Maghnouj J, et al. Decolouration of textile's effluents discoloration by adsorption in static reactor and in dynamic reactor on the phosphocalcic apatites. Phys Chem News. 2008;38:106-11.

3] Medjahed K, Tennouga L, Mansri A, Chetouani A, Hammouti B, Desbrieres J. Interaction between poly (4-vinylpyridine-graft-bromodecane) and textile blue basic dye by spectrophotometric study. Research on Chemical Intermediates. 2013;39:3199-208.

4] Gholami A, Khoshdast H, Hassanzadeh A. Applying hybrid genetic and artificial bee colony algorithms to simulate a bio-treatment of synthetic dye-polluted wastewater using a rhamnolipid biosurfactant. Journal of environmental management. 2021;299:113666.

5] Ilame T, Ghosh A. The promising applications of nanoparticles for synthetic dyes removal from wastewater: recent review. Management of Environmental Quality: An International Journal. 2022;33(2):451-77.

6] Akartasse N, Azzaoui K, Mejdoubi E, Hammouti B, Elansari LL, Abou-Salama M, et al. Environmental-friendly adsorbent composite based on hydroxyapatite/hydroxypropyl methyl-cellulose for removal of cationic dyes from an aqueous solution. Polymers. 2022;14(11):2147.

7] Amri I, Giyarsih SR. Monitoring urban physical growth in tsunami-affected areas: A case study of Banda Aceh City, Indonesia. Geojournal. 2022;87(3):1929-44.

8] N'diaye AD, Kankou MSA, Hammouti B, Nandiyanto ABD, Al Husaeni DF. A review of biomaterial as an adsorbent: From the bibliometric literature review, the definition of dyes and adsorbent, the adsorption phenomena and isotherm models, factors affecting the adsorption process, to the use of typha species waste as adsorbent. Communications in Science and Technology. 2022;7(2):140-53.

9] Donkadokula NY, Kola AK, Naz I, Saroj D. A review on advanced physico-chemical and biological textile dye wastewater treatment techniques. Reviews in environmental science and bio/technology. 2020;19:543-60.

10] Nor FHM, Abdullah S, Ibrahim Z, Nor MHM, Osman MI, Al Farraj DA, et al. Role of extremophilic Bacillus cereus KH1 and its lipopeptide in treatment of organic pollutant in wastewater. Bioprocess and Biosystems Engineering. 2023;46(3):381-91.

11] Salem SB, Mezni M, Errami M, Amine K, Salghi R, Ismat HA, et al. Degradation of enrofloxacin antibiotic under combined ionizing radiation and biological removal technologies. International Journal of Electrochemical Science. 2015;10(4):3613-22.

12] Salem IB, Errami M, Mezni M, Salghi R, Ebenso EE, Hammouti B, et al. Biological, ionizing and ultraviolet radiation and electrochemical degradation of chlorpyrifos pesticide in aqueous solutions. International Journal of Electrochemical Science. 2014;9(1):342-51.

13] Jun LY, Karri RR, Mubarak N, Yon LS, Bing CH, Khalid M, et al. Modelling of methylene blue adsorption using peroxidase immobilized functionalized Buckypaper/polyvinyl alcohol membrane via ant colony optimization. Environmental Pollution. 2020;259:113940.

14] Castel C, Favre E. Membrane separations and energy efficiency. Journal of Membrane Science. 2018;548:345-57.

15] Hassan W, Noureen S, Mustaqeem M, Saleh TA, Zafar S. Efficient adsorbent derived from Haloxylon recurvum plant for the adsorption of acid brown dye: kinetics, isotherm and thermodynamic optimization. Surfaces and Interfaces. 2020;20:100510.

16] Wei H, Gao B, Ren J, Li A, Yang H. Coagulation/flocculation in dewatering of sludge: a review. Water research. 2018;143:608-31.

17] Titchou FE, Zazou H, Afanga H, El Gaayda J, Ait Akbour R, Nidheesh PV, et al. An overview on the elimination of organic contaminants from aqueous systems using electrochemical advanced oxidation processes. Journal of Water Process Engineering. 2021;41:102040.

18] Errami M, Salghi R, Zarrouk A, Zougagh M, Zarrok H, Hammouti B, et al. Electrochemical treatment of wastewater industrial cartons. International Journal of Electrochemical Science. 2013;8(12):12672-82.

19] Zhang C, Zhang Z, He Z, Fu D. New insights into the relationship between anode material, supporting electrolyte and applied current density in anodic oxidation processes. Electrochimica Acta. 2017;229:55-64.

20] Melliti W, Errami M, Salghi R, Zarrouk A, Bazzi L, Zarrok H, et al. Electrochemical Treatment of Aqueous Wastes Agricole Containing Oxamyl By BDD-Anodic Oxidation. International Journal of Electrochemical Science. 2013;8(9):10921-31.

21] Singh AK, Hollmann D, Schwarze M, Panda C, Singh B, Menezes PW, et al. Exploring the mechanism of peroxodisulfate activation with silver metavanadate to generate abundant reactive oxygen species. Advanced Sustainable Systems. 2021;5(4):2000288.

22] Li J, Li Y, Xiong Z, Yao G, Lai B. The electrochemical advanced oxidation processes coupling of oxidants for organic pollutants degradation: a mini-review. Chinese Chemical Letters. 2019;30(12):2139-46.

23] Jiang Y, Zhao H, Liang J, Yue L, Li T, Luo Y, et al. Anodic oxidation for the degradation of organic pollutants: anode materials, operating conditions and mechanisms. A mini review. Electrochemistry Communications. 2021;123:106912.

24] Huang M, Wang X, Liu C, Fang G, Gao J, Wang Y, et al. Mechanism of metal sulfides accelerating Fe (II)/Fe (III) redox cycling to enhance pollutant degradation by persulfate: Metallic active sites vs. reducing sulfur species. Journal of Hazardous Materials. 2021;404:124175.

25] Xie J, Ma J, Zhao S, Waite TD. Flow anodic oxidation: Towards high-efficiency removal of aqueous contaminants by adsorbed hydroxyl radicals at 1.5 V vs SHE. Water Research. 2021;200:117259.

26] Badran I, Qut O, Manasrah AD, Abualhasan M. Continuous adsorptive removal of glimepiride using multi-walled carbon nanotubes in fixed-bed column. Environ Sci Pollut Res. 2021;28:14694-706.

27] Gao S, Chen Y, Su J, Wang M, Wei X, Jiang T, et al. Triboelectric nanogenerator powered electrochemical degradation of organic pollutant using Pt-free carbon materials. Acs Nano. 2017;11(4):3965-72.

28] Hamad H, Bassyouni D, El-Ashtoukhy E-S, Amin N, Abd El-Latif M. Electrocatalytic degradation and minimization of specific energy consumption of synthetic azo dye from wastewater by anodic oxidation process with an emphasis on enhancing economic efficiency and reaction mechanism. Ecotoxicology and environmental safety. 2018;148:501-12.

29] Kim J, Yeom C, Kim Y. Electrochemical degradation of organic dyes with a porous gold electrode. Korean Journal of Chemical Engineering. 2016;33:1855-9.

30] Lazar O-A, Marinoiu A, Raceanu M, Pantazi A, Mihai G, Varlam M, et al. Reduced graphene oxide decorated with dispersed gold nanoparticles: Preparation, characterization and electrochemical evaluation for oxygen reduction reaction. Energies. 2020;13(17):4307.

31] Zaaboul F, Haoufazane C, Kari A, Salim R, Azzaoui K, Sabbahi R, et al. Study of Reactive blue 203 removal by TiO2-P25 adsorption combined with photocatalysis for its degradation. Moroccan Journal of Chemistry. 2024;12(4):1664-82.

32] Sopaj F, Rodrigo MA, Oturan N, Podvorica FI, Pinson J, Oturan MA. Influence of the anode materials on the electrochemical oxidation efficiency. Application to oxidative degradation of the pharmaceutical amoxicillin. Chemical Engineering Journal. 2015;262:286-94.

33] Badran I, Al-Ejli MO. Efficient adsorptive removal of methyl green using Fe3O4/sawdust/MWCNT: Explaining sigmoidal behavior. Materials Today Communications. 2024;41:110302.

34] Thiam A, Sirés I, Garrido JA, Rodríguez RM, Brillas E. Effect of anions on electrochemical degradation of azo dye Carmoisine (Acid Red 14) using a BDD anode and air-diffusion cathode. Separation and Purification Technology. 2015;140:43-52.

35] Yue L, Wang K, Guo J, Yang J, Luo X, Lian J, et al. Enhanced electrochemical oxidation of dye wastewater with Fe2O3 supported catalyst. Journal of Industrial and Engineering Chemistry. 2014;20(2):725-31.

36] Boczkaj G, Fernandes A. Wastewater treatment by means of advanced oxidation processes at basic pH conditions: a review. Chemical engineering journal. 2017;320:608-33.

37] Cotillas S, Clematis D, Cañizares P, Carpanese MP, Rodrigo MA, Panizza M. Degradation of dye Procion Red MX-5B by electrolytic and electro-irradiated technologies using diamond electrodes. Chemosphere. 2018;199:445-52.

38] Belal RM, Zayed MA, El-Sherif RM, Ghany NAA. Advanced electrochemical degradation of basic yellow 28 textile dye using IrO2/Ti meshed electrode in different supporting electrolytes. Journal of Electroanalytical Chemistry. 2021;882:114979.

39] Nidheesh P, Zhou M, Oturan MA. An overview on the removal of synthetic dyes from water by electrochemical advanced oxidation processes. Chemosphere. 2018;197:210-27.

40] Jalife-Jacobo H, Feria-Reyes R, Serrano-Torres O, Gutiérrez-Granados S, Peralta-Hernández JM. Diazo dye Congo Red degradation using a Boron-doped diamond anode: An experimental study on the effect of supporting electrolytes. Journal of hazardous materials. 2016;319:78-83.

41] Meng X, Khoso SA, Jiang F, Zhang Y, Yue T, Gao J, et al. Removal of chemical oxygen demand and ammonia nitrogen from lead smelting wastewater with high salts content using electrochemical oxidation combined with coagulation–

flocculation treatment. Separation and Purification Technology. 2020;235:116233.

42] Soueilem SD, N'diaye AD, Abdellahi OEM, M'Baye BK, Ali YAEH, Abeidou MEKC, et al. Evaluation of the quality of boreholes water using indicators like Water Quality Index (WQI), and the Comprehensive Pollution Index (CPI). An-Najah University Journal for Research-A (Natural Sciences). 2025;39(2):None-None.

43] Sahab MF, Alani AR, Marzoog A, Fahad MM, Fayyadh AH. Utilization of Heavy Metal Pollution Indices to Appraise Surface Water Quality According to WHO Standards. An-Najah University Journal for Research-A (Natural Sciences). 2025;39(2):None-None.